

Scandium-45 NMR of pyrope-grossular garnets: Resolution of multiple scandium sites and comparison with X-ray diffraction and X-ray absorption spectroscopy

NAMJUN KIM,¹ JONATHAN F. STEBBINS,^{1,*} SIMONA QUARTIERI,^{2,3} AND ROBERTA OBERTI³

¹Department of Geological and Environmental Sciences, Stanford University, Stanford, California 94305-2115, U.S.A.

²Dipartimento di Scienze della Terra, Università di Messina, Salita Sperone 31, I-98166 Messina S. Agata, Italy

³CNR, Istituto di Geoscienze e Georisorse, unità di Pavia, via Ferrata 1, I-27100 Pavia, Italy

ABSTRACT

Here we present ⁴⁵Sc and ²⁷Al NMR results on Sc-doped pyrope (Mg₃Al₂Si₃O₁₂), grossular (Ca₃Al₂Si₃O₁₂), and an 80% grossular-20% pyrope garnet (grs80) that have recently been well-studied by X-ray diffraction and X-ray spectroscopies. Clearly distinct NMR peaks are observed for Sc in the eight-coordinated X site (pyrope and grs80) and in the six-coordinated Y site (grossular and grs80). X-ray and NMR data agree that only eight-coordinated Sc is present in pyrope and that six-coordinated Sc is predominant in grossular; however, the XRD results also indicated significant X and Z site (four-coordinated) Sc in the Ca-rich garnet. Possible reasons for this apparent discrepancy are discussed. We demonstrate that ⁴⁵Sc NMR is potentially a useful new method for studies of the site occupancies of Sc³⁺ in oxides and silicates, at least in experimental systems where its concentration is a few percent or greater.

Keywords: Crystal structure, pyrope-grossular garnet, scandium in garnet, NMR spectroscopy, pyrope-grossular garnet, scandium-45, aluminum-27

INTRODUCTION

Determination of the sites occupied by minor and trace elements in minerals is essential for physically accurate models of partitioning, solubility, diffusivity, and other properties. Among the experimental methods that are available to study local structure (as opposed to the long-range average structure obtainable by diffraction) around ions in relatively low concentrations in solid solutions, such as optical and X-ray spectroscopies, nuclear magnetic resonance (NMR) has only occasionally been used, largely because of its relatively low sensitivity. However, for relatively “favorable” nuclides, several studies have shown the ability of this technique to resolve and quantify local structural information (e.g., coordination number) for minor components in systems such as Li in beryl (Sherriff et al. 1991), B in calcite and aragonite (Sen et al. 1994), Al in MgSiO₃ perovskite, stishovite, and rutile (Stebbins et al. 2006; Stebbins 2007), Al in Ca-silicate cement minerals (Skibsted et al. 1994), and B, P, Cs, and Na sorbed onto mineral surfaces (Kim and Kirkpatrick 1997, 2004, 2006). High magnetic fields have often facilitated such studies, by enhancing sensitivity and reducing peak broadening for quadrupolar nuclides such as ¹¹B, ²³Na, and ²⁷Al.

Scandium, although rare in nature, is an interesting trace element in silicate minerals because it occurs exclusively as a trivalent cation and has a radius between those of Al³⁺ and the rare earths. It is also the lightest of the transition metals. The applications of Sc in technology are limited in part because of its high cost, but it has real interest for oxide ion conductors in fuel cells and other devices: doping with Sc³⁺ gives the highest

conductivity in the widely used family of zirconia-based ceramics (Kim et al. 2006). Sc³⁺ can be a significant element in minerals, for example in a natural scandian garnet (Galuskina et al. 2005) and in synthetic solid solutions [e.g., Ca₃Fe₂Si₃O₁₂-Ca₃Sc₂Si₃O₁₂ (Quartieri et al. 2006) and Y₃Al₂Al₃O₁₂-Y₃Sc₂Al₃O₁₂ (Tien et al. 2002) garnets]. Experimental (van Westrenen et al. 1999), theoretical (van Westrenen et al. 2003; Freeman et al. 2005), and structural (Obersti et al. 2006) studies have been made of the partitioning and substitution mechanism of Sc³⁺ (and of numerous other trace elements) in pyrope-grossular garnets.

⁴⁵Sc is, in principle, a quite favorable nuclide for solid-state NMR, having 100% natural abundance and a resonant (Larmor) frequency not far below the widely studied ²⁷Al, both leading to high sensitivity. Its relatively large quadrupolar moment ($Q = -0.22 \times 10^{28} \text{ m}^2$ vs. $0.14 \times 10^{28} \text{ m}^2$ for ²⁷Al) can lead to broad NMR peaks, as can its larger range in chemical shift and hence sensitivity of peak position to minor local structural variations induced by disorder. However, its higher nuclear spin quantum number ($I = 7/2$ vs. $5/2$ for ²⁷Al) reduces quadrupolar broadening by more than a factor of two for the same values of the quadrupolar coupling constant (C_Q). Only a few high-resolution, solid-state ⁴⁵Sc NMR studies have appeared, including a study of this nuclide in YAG (Y₃Al₂Al₃O₁₂-Y₃Sc₂Al₃O₁₂) solid solutions (Tien et al. 2002), in complex Sc-phosphates (Riou et al. 2002; Park et al. 2004), and early work on several Sc salts (Thompson and Oldfield 1987). Recently, data for several H- and F-free Sc-containing oxides were reported, which showed a rough correlation between Sc coordination number (either 6 or 8) and the isotropic chemical shift, allowing new inferences on the mean and range of Sc coordinations in Sc-doped ZrO₂ (Kim et al. 2006). In a detailed study of ⁴⁵Sc in several compounds with organic and

* E-mail: stebbins@stanford.edu

inorganic ligands, results on electric field gradient and chemical shift anisotropy tensors were reported, along with promising theoretical calculations (Rossini and Schurko 2006).

As part of a series of reports on the site partitioning and local environments of trace elements in garnets, studies of Sc-doped pyrope-grossular garnets ($\text{Mg}_3\text{Al}_2\text{Si}_3\text{O}_{12}\text{-Ca}_3\text{Al}_2\text{Si}_3\text{O}_{12}$, Oberti et al. 2006), and the $\text{Ca}_3\text{Sc}_2\text{Si}_3\text{O}_{12}\text{-Ca}_3\text{Fe}_2\text{Si}_3\text{O}_{12}$ (andradite) binary (Quartieri et al. 2006), were recently described. There, single-crystal X-ray diffraction (XRD) data, powder XRD structural refinements, and Ca and Sc X-ray absorption near-edge spectroscopy (XANES) and extended X-ray absorption fine-edge spectroscopy results were combined to present consistent pictures of Sc site distributions. In brief, it was concluded that in the andradite solutions, Sc occupied the Y-octahedral site only. However, in pyrope, Sc occupied only the X-dodecahedral site, and apparently occurred in all three cations sites in grossular, including the tetrahedral Z site. The pyrope-grossular samples (free of magnetic cations such as the Fe^{3+} in andradite) and this background information provide an excellent opportunity to evaluate and compare results from ^{45}Sc NMR, which we describe here. Spectroscopic studies and crystal chemistry of pyrope-grossular garnets in general have been reviewed in detail recently (Geiger 2004).

EXPERIMENTAL METHODS

Sc-doped garnets were synthesized by a two-step technique as described previously (Oberti et al. 2006), at 1000–1100 °C and 3–4 GPa, by adding 5 wt% Sc_2O_3 to stoichiometric pyrope-grossular starting mixtures. Samples were characterized by optical microscopy, scanning electron microscopy (SEM), XRD, and microprobe analyses (EMPA) (Oberti et al. 2006); in some powder X-ray diffractograms, the presence of one or two very weak peaks, at the limits of detectability, could suggest the presence of small amounts of an unidentified, non-garnet phase. The grossular-containing products showed some compositional heterogeneity. The compositions of the studied samples, as derived from EMPA by distributing Sc to complement the standard cations, were reported previously (Oberti et al. 2006) and are listed for convenience in Table 1. In the case of Sc-doped pyrope, a combination of EXAFS and single-crystal structure refinement gave the following, somewhat different site populations: ($\text{Mg}_{2.70}\text{Sc}_{0.30}\text{Al}_{1.00}(\text{Si}_{12.85}\text{Mg}_{0.15})\text{O}_{12}$). Samples of the end-members and of the grs80 solid solution of about 10–20 mg in weight were studied by NMR.

^{45}Sc NMR data were collected at Stanford University with Varian Unity/Inova 600 and 800 spectrometers (14.1 and 18.8 Tesla, 145.70 and 194.29 MHz), using 3.2 mm Varian/Chemagnetics “T3” MAS probes and sample spinning rates of

about 20 kHz (Kim et al. 2006). Single-pulse acquisition with typical pulse widths of 0.25 μs , which was a radiofrequency (rf) tip angle of about $\pi/24$ for the liquid reference, and pulse delays of 0.1–1 s, were chosen; because of the relatively low Sc contents, about 50000–80000 signal averages were required. Frequencies are referenced to a dilute aqueous ScCl_3 solution (about 0.02 M concentration) at 0 ppm, as in our previous report on this nuclide (Kim et al. 2006). We note that ^{45}Sc chemical shifts in more-concentrated aqueous solutions can vary significantly with composition (Melson et al. 1977); a solution of about 0.1 M concentration, chosen as the reference in another recent study (Rossini and Schurko 2006), had a chemical shift of about 1 ppm higher than our standard. ^{27}Al MAS data for the garnets were collected with the same instrument at 18.8 T (208.4 MHz) and are referenced to 0.1 M aqueous $\text{Al}(\text{NO}_3)_3$. A spinning rate of 18 kHz and 0.21 μs pulses, corresponding to a liquid rf tip angle of about $\pi/18$, were used, with pulse delays of 0.1 s and about 6000 signal averages. ^{29}Si spectra for the grossular were collected with a Varian Infinity Plus 400 system (9.4 T, 79.4 MHz) with a similar probe and were referenced to tetramethyl silane (TMS). Because of its long spin-lattice relaxation time, pulse delays of 60–300 s were used, and several thousand signal averages were collected. The small sample size still resulted in spectra with relatively low signal-to-noise ratios, however.

For the quadrupolar nuclides ^{45}Sc and ^{27}Al , the small rf tip angle chosen, and the very high magnetic field of 18.8 T, are expected to yield quantitative results for relative site populations from integrated or fitted peak areas. For the former, we recently reported accurate spectra for oxide phases with considerably higher C_Q values (broader peaks) than those estimated here, including both Sc sites in Sc_2O_3 (Kim et al. 2006). Nonetheless, as in most NMR studies of quadrupolar nuclides, it is possible that unexpectedly large C_Q values could lead to unobservably broad signals from some sites (see Discussion, below).

RESULTS

^{45}Sc NMR and Sc^{3+} site occupancies

^{45}Sc NMR spectra are shown in Figure 1. As is typical for quadrupolar nuclides, the peaks observed at 14.1 T are somewhat broader and shifted to lower frequencies than those at 18.8 T, because of greater second-order quadrupolar effects. For Sc-doped pyrope (prp in Fig. 1), a single peak is observed, centered at about 0 ppm, that shows some structure related to quadrupolar splitting but complicated (broadened) by disorder in the local Sc^{3+} structural environments inherent in the solid solution. This disorder could involve variations in Sc-O bond distances and angles, and in the local electric field gradient tensor at the Sc site, caused by varying the nature of near-neighbor site cations and the accompanying distortions of the “lattice.” Thus, none of the peaks can be accurately fitted with quadrupolar line shapes that are described by single sets of parameters. Analysis of the peak shapes and positions for Sc-doped pyrope at the two fields with the Varian STARS software package indicates a value for C_Q of about 17 ± 2 MHz, a mean quadrupolar asymmetry parameter (η , not well constrained by these data) of very roughly 0.6 ± 0.3 , and a mean isotropic chemical shift δ_{iso} of about 40 ± 5 ppm. The latter value is somewhat higher than those observed for eight-coordinated Sc in ScPO_4 and ScVO_4 (–48 and –34 ppm, respectively), but lies well below the range for six-coordinated Sc in several simple oxides (+158 to +108 ppm) (Kim et al. 2006). It is thus sensible to assign this peak to Sc in the eight-coordinated X site occupied by Mg^{2+} in pyrope.

In all of the spectra, relatively small spinning sidebands occur (spaced at the spinning frequency) that could partially mask small central peaks representing relatively low concentrations of Sc in some sites. However, because the observed sideband patterns for these spectra are symmetrical, a sideband in a region where central Sc is not expected (e.g., near to –100 ppm) can be assumed to have roughly the same shape and intensity as

TABLE 1. Sample codes and unit formulae (based on 12 O) for the samples of this work (after Table 1 in Oberti et al. 2006)

Nom. Comp.	prp (15)*	prp20grs80 (4)	prp20grs80 (5)	grs (17)	grs (6)
Oxide wt%					
MgO	27.47(33)	4.24(69)	5.69(38)	–	–
CaO	–	28.59(1.19)	28.93(14)	34.74(29)	35.18(46)
Al_2O_3	24.61(17)	20.80(35)	20.43(42)	20.15(53)	20.44(90)
SiO_2	41.73(51)	36.78(9)	39.34(71)	37.25(31)	37.59(28)
Sc_2O_3	6.78(61)	8.16(20)	4.96(1.17)	6.73(49)	5.52(27)
Total	100.58(30)	98.56(41)	99.35(30)	98.87(24)	98.72(26)

Unit formulae; Sc distributed to complete the occupancies of the normal cations

Mg	2.78	0.48	0.63	–	–
Ca	–	2.33	2.31	2.86	2.89
Sc	0.22	0.19	0.06	0.14	0.11
Al	1.97	1.86	1.80	1.83	1.85
Si	0.01	0.14	0.20	0.17	0.15
Si	2.83	2.79	2.94	2.86	2.89
Sc	0.17	0.21	0.06	0.14	0.11
Sc total	0.40	0.54	0.32	0.45	0.37

* Number of point analyses done on run products and then averaged.

those in “interesting” spectral regions (e.g., near 90 ppm) in the 18.8 T data for Sc-doped pyrope, and can be subtracted. For this sample, this shows that intensities of central peaks, other than the main X-site peak, are negligible; probably less than a few percent of the total Sc signal. The conclusion that all, or nearly all, Sc in pyrope is in the large X site is consistent with conclusions described in detail previously (Oberti et al. 2006), which were based on local Sc coordination and bond distance data from XANES and EXAFS and compositional effects on average X-O bond distances and polyhedral parameters obtained

from single-crystal XRD.

In the Sc-doped grossular sample (grs in Fig. 1), the spectra are dominated by a single, much narrower peak, which again shows broadening and distortion due to local disorder. Its shape and positions at the two fields can be approximated with mean parameters C_Q of about 12 ± 1 MHz, η of roughly 0.4 ± 0.2 , and δ_{iso} of about 115 ± 3 ppm. The latter value is well within the range known for octahedral Sc in several simple oxides (Kim et al. 2006), but is somewhat higher than reported for Sc in YAG of about 88 ppm (Tien et al. 2002). This peak can thus be unambiguously assigned to Sc in the Y site in grossular, which is predominantly occupied by Al^{3+} . Although a narrow spinning sideband occurs near to 0 ppm in the 18.8 T spectrum, there is a low, broad peak in this area as well, suggesting that a minor fraction of the Sc is in the X site as well (roughly 5% from the peak areas). All the methods applied agree that Sc is most abundant in the Y site. However, the NMR findings seem to disagree in detail with the single-crystal XRD data on a crystal selected from this material, which yielded only a slight preference for the Y site, estimated as 0.15 apfu at Y out of a total of about 0.4 apfu (Oberti et al. 2006). This discrepancy is discussed below.

In the grs80 sample, two peaks with roughly equal area are present that are similar in position and shape to the X-site peak in Sc-doped pyrope and the Y-site peak in Sc-doped grossular, although both are somewhat broadened as expected from the different local environments due to the Mg-Ca solid solution. These NMR results thus confirm the suggestions from XANES results that the solid-solution results combine the behavior detected in the two end-members (Oberti et al. 2006). The fraction of Sc observed by NMR in the X site in this sample (about 45% after subtraction of the overlapping sideband) is considerably higher than expected from a “linear mixing” of the data for the end-members. Again, this agrees with the results of the X-ray absorption spectroscopy (XAS) analysis.

At this stage of our understanding of the effects of local structure on ^{45}Sc chemical shifts, it is not feasible to make detailed comparisons between the disorder observed in NMR spectra and static or dynamic disorder (isotropic or anisotropic) observed by XRD and other methods (e.g., Geiger 2004). However, it is worth pointing out that, in general, NMR spectra (as well as XAS spectra) respond to the local structure and XRD observes the long-range average structure, which can lead to different structural descriptions. Or, if dynamical exchange of cations among sites occurs that is at a frequency much higher than the difference between their NMR resonances, NMR may also “see” a time average.

^{27}Al , ^{29}Si , and ^{45}Sc NMR: evaluation of impurity phases

Under some scenarios of Sc^{3+} substitution of into pyrope and grossular, small amounts of impurity phases could be formed during synthesis from a mixture of the end-member garnet components and Sc_2O_3 , as was done for these samples. For example, a simple substitution of Sc^{3+} for Al^{3+} in the Y site would yield a corresponding amount of excess alumina. However, if present, impurities were apparently low enough in abundance and/or small enough in size to go undetected by optical microscopy, SEM and EMPA, although powder XRD did show very weak features suggesting the presence of small amounts of unidenti-

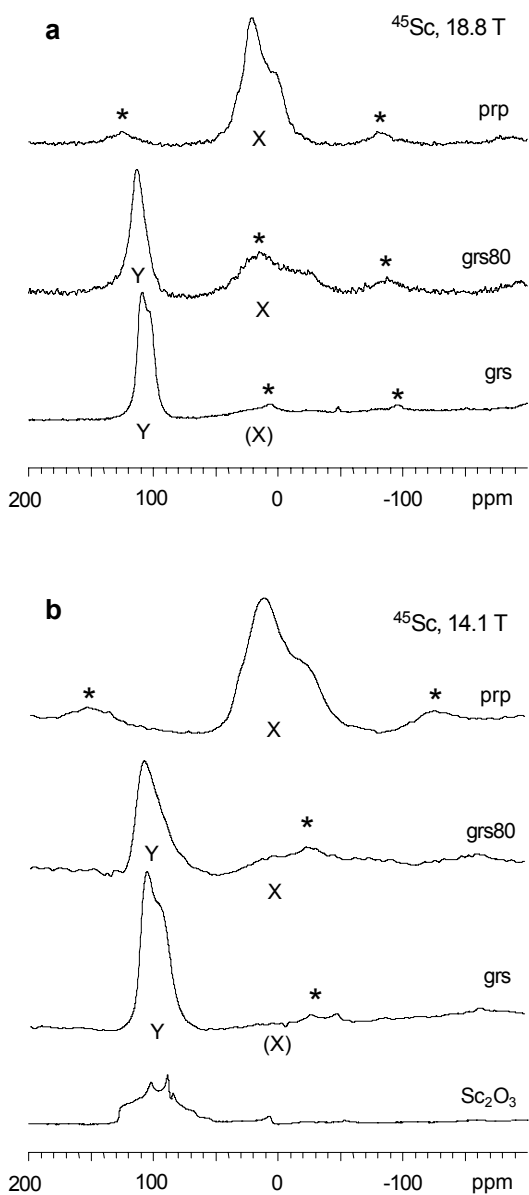


FIGURE 1. ^{45}Sc MAS NMR spectra collected at (a) 18.8 T and (b) 14.1 T fields for Sc-doped garnets and for Sc_2O_3 . Data for the latter are from (Kim et al. 2006). Asterisks mark spinning sidebands, “X” and “Y” show peaks assigned to these sites. Maximum intensities are scaled to the same arbitrary value in each spectrum.

fied non-garnet phases. We collected ^{27}Al NMR data on all three samples to help evaluate impurities, as well as ^{29}Si spectra on the grossular. The “bulk” powdered samples examined here could, of course, contain small amounts of non-garnet phases, or compositional heterogeneities, that were not present in single crystals selected for diffraction studies (Oberti et al. 2006).

As shown in Figure 2a, high-field (18.8 T) ^{27}Al spectra for the Sc-doped garnets generally closely resemble those of Sc-free garnets synthesized in a different laboratory under somewhat different P - T conditions (Kelsey et al. 2007). Each spectrum shows

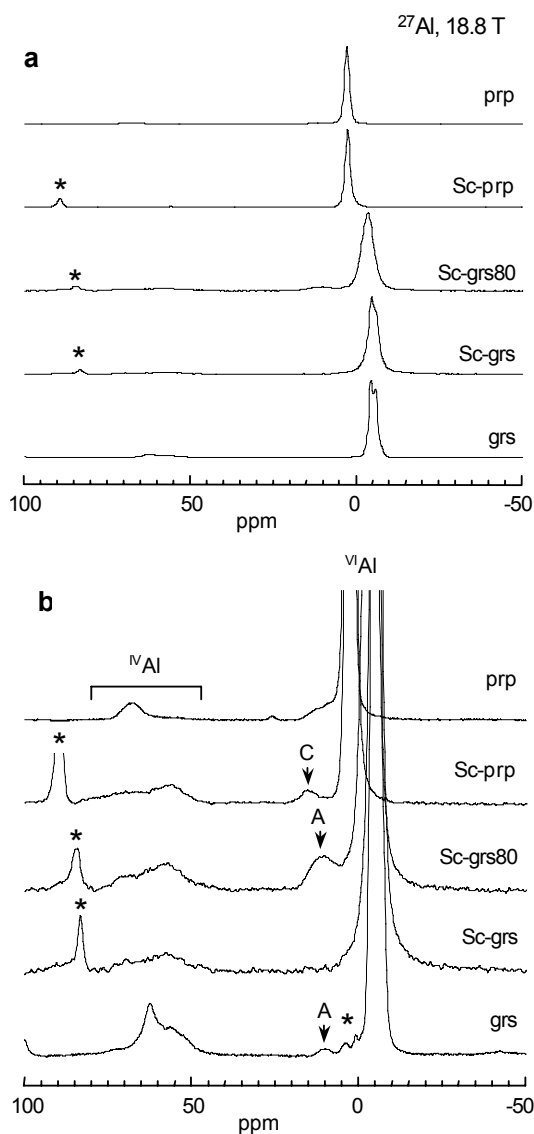


FIGURE 2. ^{27}Al MAS NMR spectra collected at 18.8 T for Sc-doped (labeled here only as “Sc-prp,” etc.) and Sc-free garnets. Data for the latter are from Kelsey et al. (2007). Asterisks mark spinning sidebands. In a, maximum intensities are scaled to the same value. In b, the same spectra are plotted, but with vertical scales magnified about 10 to 20 times, scaled so that the total peak area is the same in each. This better portrays the relative proportions of Al in the minor components such as tetrahedral Al. Regions of the spectra for 4- and 6-coordinated Al are labeled; “C” marks the peak for small amounts of corundum; “A” marks the peaks for an unknown octahedral site.

a single, narrow peak for octahedral Al whose position shifts systematically with Mg/Ca ratio. The Sc-free grossular exhibits quadrupolar splitting because of a somewhat larger C_Q value. The peaks for the Sc-doped samples are broadened somewhat, presumably by ranges (disorder) in bond distances and angles caused by the presence of Sc. In detail, the spectra for all of the samples (Sc-doped and Sc-free) show the presence of small amounts of tetrahedral Al in the form of relatively broad peaks in the region of 50 to 70 ppm. In the Sc-doped pyrope, grs80, and pure grossular, these comprise about 7, 9, and 6% of the total Al, respectively. The low intensities of the peaks and complex shapes (possibly representing multiple phases or sites) preclude detailed analysis and assignment, but it is possible that this tetrahedral Al could be present in small amounts of aluminous pyroxene, which is a common impurity phase in high-pressure garnet syntheses (Kelsey et al. 2007). The stability of CATS pyroxene in the Ca aluminosilicate system favors the development of this phase in the grs80 and grossular samples. Alternatively, small amounts of tetrahedral Al could occur in the garnets, as in Y-Al garnet (YAG), where all Y and Z sites are occupied by Al.

High-field ^{27}Al NMR is extremely sensitive to the presence of corundum, because of the narrowness of its peak, its unusually high chemical shift, and high Al content (Stebbins et al. 2006). However, of the Sc-doped garnets, only the pyrope contains detectable corundum (about 1% of the total Al signal, based on integrated peak areas), comprising less than 0.2% of the mass of the sample, given its known total Al content. Roughly 5% of the total Al signal in the spectrum for the Sc-doped, grs80 is contained in another octahedral-site peak centered at about 10 ppm of unknown origin. This feature is also present at a much lower level in Sc-free grossular.

In the pyrope, the ^{27}Al NMR data indicate that 0 to 7% of the total Al in the garnet is tetrahedral. The maximum value corresponds to 0.14 Al^{3+} per formula unit, less than half of that of the total Sc^{3+} in this sample (Oberti et al. 2006). These results support the model proposed by Oberti et al. (2006) for pyrope, where local electroneutrality is maintained by the unusual $^{\text{X}}\text{Mg}_2^{\text{X}}\text{Sc}_2^{\text{T}}\text{Si}_1^{\text{T}}\text{Mg}_1$ exchange, which was based on refined bond distances and the site-scattering value at the Z site and on the absence of Sc^{3+} incorporation at the Y site. The latter is also confirmed by present NMR data. The presence of tetrahedral Mg (which is somewhat unexpected in a high-pressure silicate) instead of twice as much tetrahedral Al, may be more effective in satisfying the geometric requirements for Sc^{3+} solution in the very compact structure of pyrope, as discussed in detail previously (Oberti et al. 2006). In contrast, the question is still open about the mechanism used to attain electroneutrality in the two grossular samples with the site occupancies suggested by the NMR data. Based on the above evidence, the incorporation of Mg at the Z site could also be suggested for the grs80 sample. In grossular, with no Mg in the system, the possibility of tetrahedral Al may be more likely, but of course the $^{\text{Y}}\text{Al}_1^{\text{Y}}\text{Sc}_1$ component of the exchange is itself charge neutral.

The ^{29}Si NMR spectrum for the Sc-doped grossular (Fig. 3) is relatively noisy because of small sample size and long spin-lattice relaxation time. The only prominent peak, at -84.0 ppm, agrees with previous studies of grossular (Bosenick et al. 1995). A small shoulder at -82.5 ppm is consistent with the presence of

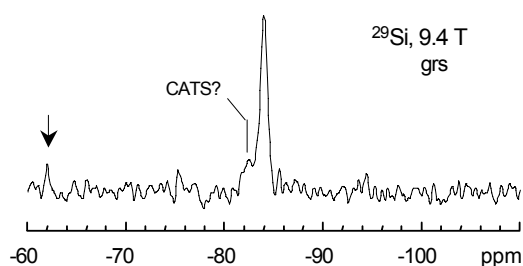


FIGURE 3. ^{29}Si MAS spectrum for Sc-doped grossular collected at 9.4 T. A peak that may be “CATS” pyroxene (Flemming and Luth 2002) is labeled; the arrow marks signal from a low-level Mg_2SiO_4 impurity in the zirconia sample rotor.

a small amount of CATS pyroxene, for which the largest peak lies at this position; the less-intense, second major peak at about -86 ppm could be lost in the noise (Flemming and Luth 2002). Given the noise level of the spectrum, though, this assignment is not definitive.

The ^{45}Sc NMR data limit the possible content of excess, undissolved Sc_2O_3 as a separate phase in the garnet samples. The two overlapped peaks for the pure oxide (corresponding to two octahedral Sc sites) are known to have sharp central singularities that do overlap with the observed Y-site Sc peaks in the garnets (Fig. 1b), but the overall peak width is about twice as large because of larger C_Q values (Riou et al. 2002; Kim et al. 2006), making it readily distinguishable. Thus, the fraction of total Sc that could be present as the oxide phase is small, probably less than 10% (0.5% of the total sample weight). This finding is consistent with the results described in Oberti et al. (2006), who noted that all or almost all Sc was incorporated into the garnet structure, based on EMPA and single-crystal XRD. If small amounts of impurity phases such as corundum or pyroxenes are present, then it is likely that these will contain some Sc in solid solution. However, unless the Sc is strongly partitioned into such phases relative to the garnets, their low abundances would preclude clear distinction of the NMR signal for the Sc that they might contain.

DISCUSSION

In recent studies by XRD and XAS methods of the same samples described here, it was concluded that in pyrope, Sc^{3+} substitutes exclusively for Mg^{2+} in the X site (Oberti et al. 2006). Evidence was presented in that paper (see above) for charge balance by substitution of Mg^{2+} for Si^{4+} in tetrahedral sites. The excess Mg and Si produced by this substitution could be present as undetected, small grains of an enstatite-rich pyroxene. The presence of sufficient Mg for this mechanism even in the grs80 solid solution may allow substantial X-site substitution of Sc^{3+} there as well, as confirmed by NMR. The ^{45}Sc NMR are consistent with this conclusion, although they do not directly demonstrate the presence of tetrahedral Mg; the ^{27}Al NMR indicates that it is possible that some (not all) charge compensation occurs through tetrahedral Al^{3+} as well, although again we emphasize that the identity of the phase(s) containing this species in these samples remains uncertain.

The ^{45}Sc NMR data suggest that most or all of the Sc^{3+} in the

grossular is present in the octahedral Y site. Crystal chemically, this isovalent substitution for Al^{3+} is the simplest mechanism, and has been well-documented by XRD and XAS studies of garnets in the $\text{Ca}_3\text{Fe}_2\text{Si}_3\text{O}_{12}$ (andradite)- $\text{Ca}_3\text{Sc}_2\text{Si}_3\text{O}_{12}$ binary where complete solid solution was found (Quartieri et al. 2006). It also agrees with the observation of a single Sc site for garnets in the $\text{Y}_3\text{Al}_2\text{Al}_3\text{O}_{12}$ (YAG)- $\text{Y}_3\text{Sc}_2\text{Al}_3\text{O}_{12}$ system (Tien et al. 2002). In both of those cases, the relatively large X cation does not substitute into the tetrahedral site as suggested for Mg^{2+} in pyrope. We note, however, that unlike the Sc-doped pyrope-grossular samples described here, those in the andradite- and YAG-containing systems were synthesized to have the appropriate binary stoichiometries (Quartieri et al. 2006; Tien et al. 2002). In the case of simple $\text{Sc}^{3+} = \text{Al}^{3+}$ substitution in grossular, an equivalent amount of alumina should be present in another phase. High-pressure phase equilibria (as well as the co-linearity of the grossular-CATS-corundum compositions) indicate that this could be an aluminous, CATS-type pyroxene (not corundum), which is at least consistent with the ^{29}Si and ^{27}Al NMR results although not uniquely confirmed by these data. In more detail, the ^{45}Sc NMR data show a minor amount of Sc^{3+} in the X site in the grossular, requiring some other charge-balancing mechanism such as a minor fraction of tetrahedral Al^{3+} .

Single-crystal X-ray structure refinements of crystals from the Sc-doped grossular sample, in terms of both refined site-scattering values and mean bond lengths, are compatible with a nearly equal partitioning of Sc^{3+} among the X, Y, and Z sites (Oberti et al. 2006). This result was in good agreement with the measured Ca, Al, and Si contents, and also obeyed local charge balance requirements. Scandium EXAFS data were not well-fitted by a model with simple substitution of Sc into the Y site of grossular, requiring a more complex model for second-shell interactions (reflecting the XRD results) but also retaining a mean first-shell coordination of six (Oberti et al. 2006).

The reasons for the apparent discrepancies between the X-ray and the ^{45}Sc NMR data on the Sc-doped grossular are not clear. There is the possibility that sample heterogeneities could lead to differences in composition between the small single crystals and the bulk powder examined by NMR, resulting in differences in structural observations. Two high-pressure runs were required to obtain the material needed for all of the data collection, but, after the “recycling” procedure used to grow larger crystals (Oberti et al. 2006), only pyrope crystals showed an excellent homogeneity, whereas Sc-grossular maintained significant heterogeneity. On the other hand, NMR studies of ^{45}Sc are still at an early stage, and correlations between structure and chemical shifts are empirical and not yet as clearly defined as for better-studied nuclides such as ^{27}Al and ^{29}Si . For example, although there seem to be relatively well-defined ranges of chemical shift for six- and eight-coordinated Sc in simple oxides, the presence of H and/or F in the structure modifies these ranges (Kim et al. 2006). It is also clear that simple correlations between mean Sc-O bond distance and chemical shift, as expected from results on a variety of other nuclides, are complicated by other ligand effects such as variations in electronegativity of first neighbor cations, e.g., vanadates vs. phosphates (Kim et al. 2006; Rossini and Schurko 2006). With respect to the particularly interesting issue of four-coordinated Sc in garnet, the apparent lack of stoichiometric

oxides with four-coordinated Sc makes this finding somewhat surprising but also obviates the collection of spectroscopic data on appropriate tetrahedral model compounds. There remains, as well, the possibility that tetrahedral Sc could be present, but that such sites are extremely distorted and have very high quadrupolar coupling constants, resulting in severely broadened NMR peaks. We note, however, that Sc sites with C_Q values much larger than those described here for the garnets (e.g., 23.4 MHz for one site in Sc_2O_3) were readily and accurately observed at 18.8 T (Kim et al. 2006) and even at 9.4 T (Riou et al. 2002).

In both natural and in experimental systems, the mechanism of solution of minor substituents in a mineral at a given temperature and pressure depends not only on the structural details of the host phase, e.g., the sizes of available cation sites and of the substituent (e.g., charge and radius), but on the overall composition of the system, which controls the activities of all of the components involved. The syntheses discussed in this and previous papers were done by adding 5% Sc_2O_3 to starting compositions of garnet stoichiometry, so that Sc incorporation was not determined in advance. Different results could be obtained starting from compositions where one major cation does not obey garnet stoichiometry, and different Sc partitioning can be expected in complex natural systems. Nonetheless, all of the NMR, XRD, and XAS data confirm that the mechanism of Sc substitution in pyrope and grossular are quite different, which will require that models for partitioning of this and related elements in geological processes take the complex effects of garnet composition into account (Oberti et al. 2006; van Westrenen et al. 2003; Freeman et al. 2005).

ACKNOWLEDGMENTS

We are grateful for support from the U.S. National Science Foundation, grant EAR 0408410, and from CNR project TA01.04.002. We thank G. Iezzi (Chieti University) for the synthesis of the Sc-doped garnets and for useful discussions of their characterization, K. Kelsey for the ^{27}Al data on the pyrope and grossular, J. Puglisi and C. Liu for access to the 18.8 T spectrometer at the Stanford Magnetic Resonance Laboratory, and Charles Geiger and two anonymous reviewers for helpful comments on the original manuscript.

REFERENCES CITED

- Bosenick, A., Geiger, C.A., Schaller, T., and Sebal, A. (1995) A ^{29}Si NMR and IR spectroscopic investigation of synthetic pyrope-grossular garnet solid solutions. *American Mineralogist*, 80, 691–704.
- Flemming, R.L. and Luth, R.W. (2002) Si-29 MAS NMR study of diopside-Ca-Tschermak clinopyroxenes: Detecting both tetrahedral and octahedral Al substitution. *American Mineralogist*, 87, 25–36.
- Freeman, C.L., Lavrentiev, M.Y., Allan, N.L., Purton, J.A., and van Westrenen, W. (2005) Similarity in silicate chemistry: trace elements in garnet solid solutions. *Journal of Molecular Structure-THEOCHEM*, 727, 199–204.
- Galuskina, I.O., Galuskin, E.V., Dzierzanowski, P., Armbruster, T., and Kozanecki, M. (2005) A natural scandian garnet. *American Mineralogist*, 90, 1688–1692.
- Geiger, C.A. (2004) Spectroscopic investigations relating to the structural crystal-chemical and lattice-dynamic properties of $(\text{Fe}^{2+}, \text{Mn}^{2+}, \text{Mg}, \text{Ca})_3\text{Al}_2\text{Si}_3\text{O}_{12}$ garnet: A review and analysis. In A. Beran and E. Libowitzky, Eds., *Spectroscopic methods in mineralogy*, 6, p. 589–645. EMU Notes in Mineralogy, Eötvös University Press, Budapest.
- Kelsey, K.E., Stebbins, J.F., Du, L.-S., and Hankins, B. (2007) Constraining ^{17}O and ^{27}Al NMR spectra of high pressure crystals and glasses: New data for jadeite, pyrope, grossular, and mullite. *American Mineralogist*, 92, 210–216.
- Kim, N., Hsieh, C.-H., and Stebbins, J.F. (2006) Scandium coordination in solid oxides and stabilized zirconia: ^{45}Sc NMR. *Chemistry of Materials*, 18, 3855–3859.
- Kim, Y. and Kirkpatrick, R.J. (1997) Na-23 and Cs-133 NMR study of cation adsorption on mineral surfaces: Local environments, dynamics, and effects of mixed cations. *Geochimica et Cosmochimica Acta*, 61, 5199–5208.
- (2004) An investigation of phosphate adsorbed on aluminum oxyhydroxide and oxide phases by nuclear magnetic resonance. *European Journal of Soil Science*, 55, 243–251.
- (2006) B-11 NMR investigation of boron interaction with mineral surfaces: Results for boehmite, silica gel and illite. *Geochimica et Cosmochimica Acta*, 70, 3231–3238.
- Melson, G.A., Olszanski, D.J., and Rahimi, A.K. (1977) Coordination chemistry of scandium. VIII. Detection of complex formation in solution by ^{45}Sc NMR spectroscopy. *Spectrochimica Acta*, 33A, 301–309.
- Oberti, R., Quartieri, S., Dalconi, M.C., Boscherini, F., Iezzi, G., Boiocchi, M., and Eeckhout, S.G. (2006) Site preference and local geometry of Sc in garnets: Part I. Multifarious mechanisms in the pyrope-grossular join. *American Mineralogist*, 91, 1230–1239.
- Park, H.S., Bull, I., Peng, L.M., Victor, G.Y.J., Grey, C.P., and Parise, J.B. (2004) Synthesis and structure determination of a new organically templated scandium fluorophosphate framework and its indium analog. *Chemistry of Materials*, 16, 5350–5356.
- Quartieri, S., Oberti, R., Boiocchi, M., Dalconi, M.C., Boscherini, F., Safonova, O., and Woodland, A.B. (2006) Site preference and local geometry of Sc in garnets: Part II. The crystal-chemistry of octahedral Sc in the andradite- $\text{Ca}_2\text{Sc}_2\text{Si}_2\text{O}_{12}$ join. *American Mineralogist*, 91, 1240–1248.
- Riou, D., Fayon, F., and Massiot, D. (2002) Hydrothermal synthesis, structure determination, and solid state NMR study of the first organically templated scandium phosphate. *Chemistry of Materials*, 14, 2416–2420.
- Rossini, A.J. and Schurko, R.W. (2006) Experimental and theoretical studies of ^{45}Sc NMR interactions in solids. *Journal of the American Chemical Society*, 128, 10391–10402.
- Sen, S., Stebbins, J.F., Hemming, N.G., and Ghosh, B. (1994) Coordination environments of B impurities in calcite and aragonite polymorphs: A ^{11}B MAS NMR study. *American Mineralogist*, 79, 819–825.
- Sherriff, B.L., Grundy, H.D., Hartman, J.S., Hawthorne, F.C., and Cerny, P. (1991) The incorporation of alkalis in beryl: Multi-nuclear MAS NMR and crystal-structure study. *Canadian Mineralogist*, 29, 271–285.
- Skibsted, J., Jakobsen, H.J., and Hall, C. (1994) Direct observation of aluminum guest ions in the silicate phases of cement minerals by ^{27}Al MAS NMR spectroscopy. *Journal of the Chemical Society, Faraday Transactions*, 90, 2095–2098.
- Stebbins, J.F. (2007) Aluminum substitution in rutile titanium dioxide: New constraints from high-resolution ^{27}Al NMR. *Chemistry of Materials*, 19, 1862–1869.
- Stebbins, J.F., Du, L.-S., Kelsey, K., Kojitani, K., Akaogi, M., and Ono, S. (2006) Aluminum substitution in stishovite and MgSiO_3 perovskite: High-resolution ^{27}Al NMR. *American Mineralogist*, 91, 337–343.
- Thompson, A.R. and Oldfield, E. (1987) Solid-state scandium-45, yttrium-89, and lanthanum-139 NMR spectroscopy. *Journal of the Chemical Society, Chemical Communications*, 27–29.
- Tien, C., Charnaya, E.V., Sun, S.Y., Wu, R.R., Ivanov, S.N., and Khazanov, E.N. (2002) ^{27}Al and ^{45}Sc NMR studies of the $\text{Y}_2\text{ScAl}_3\text{O}_{12}$ mixed garnets. *Physica Status Solidi (b)*, 233, 222–229.
- van Westrenen, W., Blundy, J.D., and Wood, B.J. (1999) Crystal-chemical controls on trace-element partitioning between garnets and anhydrous silicate melts. *American Mineralogist*, 84, 838–847.
- van Westrenen, W., Allan, N.L., Blundy, J.D., Lavrentiev, M.Y., Lucas, B.R., and Purton, J.A. (2003) Trace element incorporation into pyrope-grossular solid solutions: an atomistic simulation study. *Physics and Chemistry of Minerals*, 30, 217–229.

MANUSCRIPT RECEIVED FEBRUARY 7, 2007

MANUSCRIPT ACCEPTED JULY 4, 2007

MANUSCRIPT HANDLED BY MICHAEL FECHTELKORD